Vertical Current Density Structure of Saturn's Equatorial Current Sheet

C. J. Martin[1], C. S. Arridge[1], N. A. Case[1], L. C. Ray[1]

[1]Physics Department, Lancaster University, Bailrigg, Lancaster, LA1 4YB, United Kingdom.

Key Points:

- Aperiodic waves on Saturn's current sheet are utilised to estimate the current density profile.
- The average full time derivative of the component of magnetic field in the exterior field direction is used to infer the current density.
- 10% of the time we sample Saturn's magnetospheric current sheet it is bifurcated, which is lower than the occurrence rate at Earth.

Corresponding author: C. J. Martin , c.martin1@lancaster.ac.uk

Abstract

Routine spacecraft encounters with the Saturn current sheet due to the passage of aperiodic waves provide the opportunity to analyse the current sheet structure. The current density is expected to peak where the field strength reaches a minima if approximated as a Harris current sheet. However, in Earth's magnetotail that this is not always the case as the sheet is sometimes bifurcated (having two or more maxima in the current density). We utilise measurements of Saturn's magnetic field to estimate the current density during crossings of the current sheet by time differentiating the B_a component of the field in a current sheet coordinate system, where B_a is perpendicular to both the current and current sheet normal. This is then averaged and organised by the magnitude of B_a. Using this method, we can identify a classical Harris-style or bifurcated current sheet as a peak at the centre or two distinct maxima on either side of $B_a = 0$, respectively. We find that around 10% of current sheet profiles exhibit a bifurcated current sheet signature, which is substantially lower than a ~25% occurrence rate at Earth.

1 Introduction

The equatorial current sheet at Saturn is a result of a rotationally dominated system [*Southwood & Kivelson*, 2001] with internal plasma sources such as Enceladus and the other moons, the rings and even the planet itself [e.g. *Pontius et al.*, 2006; *Tokar et al.*, 2005; *Jurac et al.*, 2002; *Felici et al.* , 2016]. The internal plasma and fast rotation result in centrifugal stresses [*Arridge et al.*, 2007] that cause the planet's magnetic field to stretch outwards at the equator. This ballooning forms a washer shaped current sheet (much like Earth's cross tail current sheet). Unlike Earth, however, Saturn's current sheet can be found in all local time sectors, except near noon during compressions due to solar wind dynamic pressure [*Arridge et al.*, 2008b]. The a thin current sheet extends outward from $\sim$ 15 R_S (Saturn Radii = 58,232 km) where pressure gradients and the magnetic tension force become dominated by centrifugal stresses [*Arridge et al.*, 2007].

Sergis et al. [2017] mapped the equatorial current density in Saturn's inner magnetosphere from 5-16 R_S, showing that the particle pressure is dominated by hot plasma pressure (hot ions) outside of 12 R_S with a number of local time effects. *Kellett et al.* [2011] detailed the local time and temporal variability of the current density using Cassini's equatorial orbits between 2005 and 2006. The current is strongest from dusk to midnight and can vary temporally by a factor of 2-3. In the middle to outer magnetosphere, the current density increases

from pre-midnight to pre-noon and forms a region-2-like current system [*Martin & Arridge*, 2018].

A number of studies have shown that the current sheet exhibits predictable quasi-static features, such as flapping at the rotation rate of the planet [e.g. *Provan et al.*, 2012; *Arridge et al.*, 2011]. The current sheet also forms a seasonal bowl shape [*Arridge et al.*, 2008a] and also displays random movements associated with single waveforms travelling along the sheet [*Martin & Arridge*, 2017]. These waves are solitary movements which kink the sheet as they travel. Some local time dependence of the thickness of the current sheet can be attributed to the magnetic field being more dipolar through noon or due to ambipolar magnetic fields [e.g. *Krupp et al.*, 1999; *Kellett et al.*, 2009; *Arridge et al.*, 2015; *Martin & Arridge*, 2017].

The current sheet is also thought to vary in thickness due to oscillations near the planetary rotation rate [*Thomsen et al.*, 2016]. However, it is commonly assumed that the current density peaks at the centre of the current sheet and that the current sheet magnetic field exhibits Harris-like behaviour where the magnetic field increases as a hyperbolic tangent function away from the centre, and the current density decreases exponentially away from the centre. Whilst this assumption is necessary for a number of analysis techniques, it might fail. In this study we will test whether the assumption of a Harris-like current sheet at Saturn is a discriminative or restrictive assumption to make. Throughout, we refer to 'Harris-like' current sheets, this refers to a current sheet in which the current density peaks where the magnetic field passes through one minimum and is not necessarily a strictly Harris current profile [*Harris*, 1962].

Bifurcation, or splitting of the current into two maxima of current that do not lie at the expected current sheet centre, is a common occurrence in Earth's magnetotail. First observed by *Hoshino et al.* [1996] using single spacecraft measurements and by *Runov et al.* [2003a] using the Cluster mission. Around 25% of all current sheets encounters exhibit bifurcated behaviour [*Thompson et al.*, 2006]. A dependance on the magnitude of V_x (velocity along Earth-Sun line) in the tail is found by *Asano et al.* [2005], where up to 50% of 'fast' events, and around 10% of 'not-fast' events show bifurcations. A number of authors show, with spacecraft data and models of the current sheet, that bifurcation in the tail current sheet is a precursor to, or a result of reconnection occurring [e.g. *Hoshino et al.*, 1996; *Nakamura et al.*, 2002; *Thompson et al.*, 2006; *Birn & Hesse*, 2014]. More recently, bifurcation of the

current sheet has been linked to substorm onset and an increase in current density in the tail current sheet [*Saito*, 2015].

Models have shown that a bifurcated current sheet can be caused by a number of instabilities [*Ricci et al.*, 2004; *Camporeale & Lapenta*, 2005; *Génot et al.* , 2005; *Matsui & Daughton*, 2008; *Zelenyi et al.*, 2002, 2003; *Delcourt et al.*, 2006] such as the lower hybrid drift instability, and Kelvin-Helmholtz instabilities. These instabilities may be related to increased reconnection [*Runov et al.*, 2003b; *Mok et al.*, 2006] and flapping motions of the current sheet [*Sitnov et al.*, 2004; *Runov et al.*, 2003a].

Perpendicular anisotropies in the ion temperature have been shown to form bifurcated current sheets in models and in Cluster observations of the terrestrial magnetic field and plasma [*Sitnov et al.*, 2003, 2004; *Israelevich & Ershkovich*, 2008]. *Dalena et al.* [2010] specifically focused on the role of oxygen ions in these anisotropies that may also cause instabilities and hence, bifurcation. Simulations have shown that bifurcations can be formed by perturbations in the dipole field [*Sitnov & Merkin*, 2016]. Altogether, we can assume that the bifurcation of the current sheet at Earth is linked to an unstable current sheet caused by a number of the above described processes.

At Earth, most studies make use of Cluster 4-point measurements to determine current density, however, at Jupiter and Saturn single space craft measurements and other methods must be used. Bifurcated current sheets at Jupiter have previously been investigated using the full time derivative of the magnetic field component perpendicular to both the direction of current flow and the current sheet normal [*Hoshino et al.*, 1996; *Israelevich & Ershkovich*, 2006]. Several examples of bifurcated sheets were found using Voyager-2 and Galileo magnetometer data [*Israelevich & Ershkovich*, 2008]. The authors concluded that the bifurcation is due to an ion pressure anisotropy perpendicular to the magnetic field. The total number of bifurcated sheets detected is very small compared to the total number of current sheet crossings, suggesting that this is a very rare phenomenon at Jupiter. The difference in the bifurcated and non-bifurcated ratio between Earth's tail current sheet and Jupiter's current sheet is likely caused by the different ion distribution functions, initially due to the differing processes of plasma transport that create the plasma sheet [*Israelevich & Ershkovich*, 2008].

To investigate the proportion of bifurcated sheets at Saturn, we utilise the aperiodic wave structures [*Martin & Arridge*, 2017] that cause Cassini to encounter the current sheet. The overall flapping motion of Jupiter's magnetosphere, due to the offset of the magnetic

axis from the rotational axis, allows for periodic sampling of the current sheet at Jupiter. This process does not occur at Saturn due to a near alignment of the magnetic and rotational axes[*Acuña & Ness*, 1980; *Smith et al.*, 1980; *Dougherty et al.*, 2018], and so we do not get constant periodic sampling of the current sheet. We note that the planetary period oscillations allow for current sheet flapping [*Arridge et al.*, 2011; *Provan et al.*, 2012], however this does not frequently result in the sampling of both lobes but acts instead to move the current sheet towards and away from Cassini without a direct encounter.

The aperiodic waves are detected using Cassini magnetometer data [*Dougherty et al.*, 2004], and appear as a traversal from one lobe to the other and back again to the original lobe. We consider waves that have a period of less than the global flapping waves (most waves have time periods of from 1-30 minutes), are non-repeating (solitary) and have a deflection in the radial magnetic field of over 1 nT. The waves kink the field as they travel in a predominantly outward radial direction. All events occur planet-ward inside of the magnetopause boundary, which is found by manual examination of the magnetic field data. The magnetic field magnitude and direction describe the regime in which Cassini resides, and hence a boundary between two regimes can be established by examining the changes in these parameters, i.e. the magnetosheath generally has a smaller magnitude than the current sheet and lobes. The direction of lobe magnetic field is mainly radial, whereas the current sheet has a predominantly north-south component. Between January 2005 to December 2012, 1461 events fit these criteria from the equatorial revolutions of Cassini. For further analysis of aperiodic wave properties and applications, the authors direct the reader to *Martin & Arridge* [2017, 2018].

2 Method

Firstly, we must rotate the magnetic field into a current sheet coordinate system (A,B,C) where $\hat{\boldsymbol{a}}$ is positive in the direction of largest change in magnetic field (roughly in the positive radial direction), $\hat{\boldsymbol{c}}$ is normal to the current sheet and $\hat{\boldsymbol{b}}$ completes the right handed system and is in the direction of the current density vector. A representation of the two coordinate systems can be found in figure 1. To rotate the original coordinates we must first find the normal to the current sheet which is done using a number of methods. We first find a normal using minimum variance analysis (MVA), where we can use single spacecraft data to estimate the direction of minimum variance which is the normal to an approximately one-dimensional current layer [*Sonnerup & Cahill*, 1967].

144 However, if the variance ellipsoid (a 3-dimensional representation of the variance of
145 the data in space) is degenerate such that we cannot separate the minimum and intermediate
146 eigenvectors, then the uncertainty of the normal placement is high. In such cases, we then
147 use a second method of finding the normal to reduce the uncertainty in the normal direc-
148 tion. This second method, the coplanarity method, calculates the difference in northern and
149 southern lobe fields ($\Delta\boldsymbol{B}$) and the cross product of the northern lobe magnetic field and the
150 southern lobe magnetic field, ($\boldsymbol{B_N} \times \boldsymbol{B_S}$). As both of these vector products are in the plane of
151 the current sheet, the cross product $\Delta\boldsymbol{B} \times (\boldsymbol{B_N} \times \boldsymbol{B_S})$ will be in the normal direction of the
152 current sheet.

153 We initially use MVA to determine the normal direction as the uncertainties ascer-
154 tained using a bootstrapping method are on average much smaller than the uncertainties
155 found when using the coplanarity method, under the assumption that the minimum and inter-
156 mediate variance directions are not degenerate. Uncertainties in the coplanarity method are
157 determined using the standard deviation of the mean values of $\boldsymbol{B_N}$ and $\boldsymbol{B_S}$, which are then
158 propagated to give an uncertainty on the variance directions. In the computational algorithm,
159 we use coplanarity when we find that the MVA uncertainties are larger than the coplanarity
160 uncertainties and/or the MVA analysis is degenerate. An additional feature of MVA is that
161 the maximum variance direction is equivalent to the direction of $\Delta\boldsymbol{B}$, which can be used as
162 a check for both methods as the maximum variance is often the least degenerate and most
163 accurately calculated variance direction. In examples where both methods of finding the co-
164 ordinate system give acceptable uncertainties, the results are in agreement.

165 Once we have the normal direction, we can establish the angles needed to rotate the
166 magnetic field into the new (A,B,C) co-ordinate system described above. These angles (α, β, γ)
167 give the angles in three planes of the normal from the radial direction for α and β, and from
168 the ϕ direction for γ. Hence, we now have our new co-ordinate system ordered by the current
169 sheet of Saturn.

170 We focus now on the magnetic field in $\hat{\boldsymbol{a}}$, or B_a. B_a is not only time dependent but also
171 dependent on the position of the current sheet $B_a(t) \approx B_a(c(t))$ and hence the full derivative
172 is:

$$\frac{dB_a}{dt} = \frac{\partial B_a}{\partial c}\frac{dc}{dt}, \tag{1}$$

173 For an aperiodic wave we find that $\left\langle \frac{dc}{dt} \right\rangle$ will equal zero over the course of one wave, assum-
174 ing the current sheet returns to its original position and the spacecraft does not move during

this time. Hence, $\langle \frac{dB_a}{dt} \rangle \approx 0$. Through Ampère's law, we know that $\frac{\partial B_a}{\partial c}$ is proportional to the current density in the sheet and so organising $\langle |\frac{dB_a}{dt}| \rangle$ versus B_a will show the peak in current density as Cassini measures the centre of the current sheet (assuming a Harris-like current sheet). A Harris-like current sheet will show a peak in $\langle |\frac{dB_a}{dt}| \rangle$ at $B_a = 0$ whereas a bifurcated current sheet will show two peaks either side of $B_a = 0$. Additionally, we note that these may be shifted from the zero line due to global motion of the current sheet that cannot be accounted for in this analysi, i.e. $\langle \frac{dB_a}{dt} \rangle \neq 0$. Most aperiodic waves occur on small timescales, and thus we can neglect global motion effect on a zero shift.

At Jupiter, *Israelevich & Ershkovich* [2006] calculated the differential value using a number of crossings and the assumption $\langle \frac{dc}{dt} \rangle = 0$ is held for regular flapping motion since Galileo was an equatorial orbiter. However, at Saturn, Cassini covers a large range of latitudes and we cannot assume that the periodic oscillations will result in $\langle \frac{dc}{dt} \rangle = 0$. Using aperiodic waves allows for this assumption to be satisfied as the aperiodic waves sample both lobes, and the time series of magnetometer data for a single aperiodic wave can be restricted so that there is equivalent sampling of both magnetic lobes of Saturn.

$\frac{dB_a}{dt}$ is calculated numerically by $[B_a(t + \Delta t) - B_a(t - \Delta t)]/2\Delta t$, where in this study $\Delta t = 1$ second. We bin the differential into B_a bins of size 0.1 - 0.25 nT to allow for at least reasonable number of data points ($N > 10$) in each bin for each aperiodic wave. Hence we can now relate a proxy for current density with a proxy for the distance from the centre of the current sheet (B_a).

To test whether we find a bifurcated, Harris-like or unclassified current density profile, we used a model made up of three Gaussian distributions. The first Gaussian is centred on a 'centre' value (C) or close to $B_a = 0$, the second and third Gaussians are centred on an 'offset' from the centre (ω), on either side (C - ω and C + ω). All distributions share the same 'spread' (σ), the central Gaussian has an independent amplitude (A_{Harris}) to the peripheral Gaussians ($A_{Bifurcated}$). Hence, if we find a Harris-like current sheet, we expect the central Gaussian to have a considerably larger amplitude than the peripheral Gaussians, and vice versa for a bifurcated signature.

This model is fitted to $\langle |\frac{dB_a}{dt}| \rangle$ vs B_a as described above using Bayesian regression analysis, where prior knowledge of the probable outcome is used to give a probability distribution of the final result. We find that the use of Bayesian regression analysis allows for a much more in-depth analysis of the uncertainties of the fitting of the model, this method

of fitting easily shows any covariance between the variables. Each unknown (C,ω,σ, A_{Harris} and $A_{Bifurcated}$) is given a prior distribution, which for C_{prior} is a normal distribution around $B_a = 0$, ω_{prior} and σ_{prior} are positive only distributions with decreasing probability with larger offsets and spreads. Both amplitude priors are given as a positive only normal distribution around the median value of $\langle|\frac{dB_a}{dt}|\rangle$. These prior distributions are then multiplied by a likelihood distribution based on finding the lowest χ^2 value when comparing the data to 100,000 randomly distributed samples taken from the prior distributions. The output for this method is hence a 'posterior' distribution of each fitted parameter which peaks at the most likely value and shows a spread (and hence uncertainty) in that value.

To algorithmically determine whether the profile is Harris-like or bifurcated, we implement a number of criteria. To be bifurcated the distribution must have an $A_{Bifurcated}$ of at least 1.5 times an A_{Harris}. Additionally, the offset (ω) must be more than twice the spread (σ) and the absolute centre value (C) must be less than the offset (ω) value. To be considered a Harris-like sheet the criteria are as follows: an A_{Harris} of at least 1.5 times an $A_{bifurcated}$; σ must be less than twice the offset (ω); and the absolute centre value (C) must be less than the offset (ω). Distributions that do not comply with either criterions are considered unclassified and are visually inspected. Distributions that are borderline on either classification are also visually inspected as a secondary check.

This method of fitting variables is useful to find the interconnectivity of the variable themselves. We may find a dependence of one variable on another, and if this is found then the model must be updated or revised to remove this dependance. In this study, the majority of events lead to the conclusion that the variables fitted are independent of each other, and any case of strong dependence is removed from further analysis.

3 Results

The normal vector can be found using either MVA or coplanarity in 1018 out of 1461 aperiodic wave events, of these events 807 sample an adequate amount of both lobes to build up an acceptable picture of the current density profile. We find 79 bifurcated signatures and 632 Harris-like signatures. From the total, 96 events give a striated, unclassified or ambiguous signature. Thus we find that 10% of current sheet profiles at Saturn are bifurcated, 78% of profiles show a Harris-like current sheet and 12% of current sheets show a unclassified signature.

Figure 2 shows an example of a Harris-like current sheet signature for Saturn's equatorial current sheet. The dotted line shows the mean value of $\langle|\frac{dB_a}{dt}|\rangle$ and the error bars give the standard deviation in each B_a bin. An orange solid line shows the most likely fitted distribution from the Bayesian inference algorithm described in the previous section. Figure 3 shows an example of a bifurcated current sheet. Figure 4 shows an example of an unclassified/ambiguous profile.

Figure 5 shows the distribution of bifurcated and Harris-like current sheets around Saturn, with nominal magnetopause positions, Titan's orbit at 20 R_S and Rhea's orbit at 9 R_S. Figure 5 a) shows the total number of aperiodic wave events in the magnetosphere, we see an asymmetry in dawn and dusk where a larger number are found along the dusk flank. Overall, we can assume that the number of events in each area of the magnetosphere scale with the time spent there by Cassini. 5 b) shows the number of bifurcated current sheets normalised by the total number of aperiodic wave events (and hence takes into account Cassini's trajectory bias). We see a large asymmetry between dawn and dusk where no bifurcated signatures are seen in the dawn sector outside of Titan's orbit.

In comparison, figure 5c), shows the number of Harris-like current sheets normalised to the total number of aperiodic waves. To compare, we divide the number of bifurcated sheets by the number of Harris-like current sheets to find the ratio of Bifurcated and Harris-like sheets (5 d) where 1 is Harris-like dominated, and -1 is bifurcated dominated. As Harris-like sheets are dominant, the plot shows mainly red values (+1). However, we also see the asymmetry shown in 5 a) with no bifurcation in the dawn section, and around double the number of Harris-like sheets than bifurcated sheets in the dusk sector. We show the number of striated and NaN (undefined number) and NED (not enough data) current sheets for completeness in 5e and f, both are normalised to the total number of events.

Spatially, we find no strong correlation with radial distance or Saturn local time when normalised to the distributions of the entire catalogue of events for the Harris-like or unclassified. The only deviation from the distribution of all events is a lack of any bifurcated signatures outside of 20 R_S in the dawn flank, which may be linked to a more stable and on average thinner current sheet in this area [e.g. *Kellett et al.* [2009], *Kidder et al.* [2009] & *Giampieri et al.* [2004]].

4 Discussion

The vertical structure of current density in Saturn's equatorial current sheet is explored using Cassini magnetometer measurements during aperiodic wave events. The structure is inferred from calculating the full time derivative of the magnetic field in the *a* direction in a current sheet coordinate system. Harris-like, bifurcated and unclassified sheets are found to be in proportions of 78%, 10% and 12%, respectively. These proportions are insensitive to changes in the criteria of classification.

At Earth, approximately 25% of current sheets examined are bifurcated [*Thompson et al.*, 2006], however *Asano et al.* [2005] showed that a dependence on velocity along the Earth-sun line was a factor in the number of bifurcated current sheets found. At high velocities (>500 km/s), bifurcated and Harris-like were proportioned at 50% / 50% whereas at lower velocities (<300 km/s) the distribution of Harris-like sheets to bifurcated sheets is much lower at 90% /10% - a ratio nearer to the values found in this study.

A general consensus on bifurcated current sheets at Earth is that they are caused by a perturbation or instability of the current sheet. One example is tail reconnection occurring during substorms at Earth, where the reconnection is constrained in local time to near midnight. At Saturn, the equatorial current sheet is present in all local times (given solar wind conditions) and hence reconnection can occur in all local times [*Guo et al.* , 2018]. As bifurcation happens at Saturn in most local time sectors, reconnection and associated phenomena could be the causes of the splitting of the current density. We find a small increase in bifurcation occurrence in the post-midnight sector, where we expect the x-line from reconnection in the Vasyliunas cycle to be situated, hence giving additional credence to this theory.

Delamere et al. [2015] suggest that a 'patchy network of reconnection sites' along the magnetopause may be responsible for small-scale losses of plasma in the noon sector through to the dusk sector of Saturn's magnetosphere. This area is also where an increased number of bifurcated current sheets are found, and as such plasma instabilities caused by the patchy reconnection my be attributed to the larger number of bifurcated current sheet detected. Pressure anisotropies are also found in the nightside current sheet at Jupiter, showing that the pressure parallel to the field was greater than the pressure perpendicular during the Voyager 1 and 2 flybys [*Paranicas et al.*, 1991]. However, at present, the plasma instabilities and anisotropies are not fully understood at the outer planets and as such, a definitive conclusion for the sources for the bifurcation cannot be made.

5 Summary

In this study the vertical structure of Saturn's equatorial current sheet is explored using the single-spacecraft method from *Israelevich & Ershkovich* [2006] combined with a Bayesian regression analysis. Due to the lack of an appreciable dipole tilt, current sheet encounters during the passage of aperiodic waves [*Martin & Arridge*, 2017] are used to obtain the profile of the magnetic field through the current sheet. Through each current sheet encounter the full time derivative of the B_a component of the field was binned as a function of B_a. A simple model based on the sum of Gaussians is used to identify profiles with a current density peak near the centre of the current sheet (Harris-like) or with off-centre peaks. Model parameters were obtained via Bayesian inference. We find that 78% of the current sheet profiles show a Harris-like structure, 10% are bifurcated, and 12% are unclassified. This compares with 25% in Earth's magnetotail.

Phenomenologically, at Earth bifurcated current sheets are more often found during fast flow events and are associated with substorms [*Saito*, 2015], thus related to magnetic reconnection. Theory and simulations have explored the role of instabilities or plasma anisotropy that can give-rise to bifurcations. We must also discuss the possibility of the aperiodic waves themselves affecting or being affected by the bifurcation or source of bifurcation. Fast flows in the current sheet sheet may inhibit the kinking of the current sheet during the passage of a wave, and so would limit the amplitude of the wave. Additionally, passage of an aperiodic wave may modify the current sheet to encourage or inhibit reconnection through changes in the stress balance. We have insufficient information of the role of these processes at Saturn to definitively identify the process and its impact on both aperiodic waves and bifurcation.

Future observational work should focus on attempting to identify correlations of bifurcated current sheets with faster flows/reconnection events at Saturn, and studying the plasma/energetic particle differences between Harris-like and bifurcated current sheets. More detailed surveys of the jovian system should also be carried out to statistically determine the prevalence of bifurcated current sheets at Jupiter. There is also theoretical and simulation work that can be done to examine the generation of bifurcations for conditions compatible with Saturn and Jupiter.

Acknowledgments

C.J.M. was funded by a Faculty of Science and Technology studentship from Lancaster University. C.S.A. was funded by a Royal Society Research Fellowship and STFC grant number ST/R000816/1. L.C.R & N.A.C. were supported during this study by STFC grant number ST/R000816/1. Cassini MAG data used in this study may be obtained from the Planetary Data System (http://pds.nasa.gov/).

References

Acuña, M.H. and Ness, N.F., (1980). The magnetic field of Saturn: Pioneer 11 observations. *Science*, *207*(4429), 444-446. doi:10.1126/science.207.4429.444

Arridge, C. S., Russell, C. T., Khurana, K. K., Achilleos, N., Andre, N., Rymer, A. M., Dougherty, M. K., Coates, A. J., (2007). Mass of Saturn's magnetodisc: Cassini observations, *Geophysical Research Letters*, *34*(A11), 8779–8789, doi:10.1029/2006GL028921

Arridge, C.S., Khurana, K.K., Russell, C.T., Southwood, D.J., Achilleos, N., Dougherty, M.K., Coates, A.J. and Leinweber, H.K., (2008a). Warping of Saturn's magnetospheric and magnetotail current sheets, *Journal of Geophysical Research: Space Physics*, *113*(A8), 2156–2202, doi:10.1029/2007JA012963

Arridge, C.S., Russell, C.T., Khurana, K.K., Achilleos, N., Cowley, S.W.H., Dougherty, M.K., Southwood, D.J. and Bunce, E.J., (2008b). Saturn's magnetodisc current sheet. *Journal of Geophysical Research: Space Physics*, *113*(A4), doi:10.1029/2007JA012540

Arridge, C. S., André, N., Khurana, K. K., Russell, C. T., Cowley, S. W. H., Provan, G., Andrews, D. J., Jackman, C. M., Coates, A. J., Sittler, E. C., Dougherty, M. K., Young, D. T. (2011) Periodic motion of Saturn's nightside plasma sheet *Journal of Geophysical Research*,*116*, doi:10.1029/2011JA016827

Arridge, C. S., Kane, M. , Sergis, N., Khurana, K. K., Jackman, C. J., (2015) Sources of local time asymmetries in magnetodiscs *Space Science Reviews*, *187*, 301–333, doi:10.1007/s11214-015-0145

Asano, Y., Nakamura, R., Baumjohann, W., Runov, A., Vörös, Z., Volwerk, M., Zhang, T.L., Balogh, A., Klecker, B. and Reme, H., (2005). How typical are atypical current sheets?. *Geophysical Research Letters*, *32*(3), doi:10.1029/2004GL021834

Birn, J. and Hesse, M., 2014. Forced reconnection in the near magnetotail: Onset and energy conversion in PIC and MHD simulations. *Journal of Geophysical Research: Space Physics*, *119*(1), pp.290-309, doi:10.1002/2013JA019354

Camporeale, E. and Lapenta, G., (2005). Model of bifurcated current sheets in the Earth's magnetotail: Equilibrium and stability. *Journal of Geophysical Research: Space Physics*, *110*(A7), doi:10.1029/2004JA010779

Dalena, S., Greco, A., Zimbardo, G. and Veltri, P., (2010). Role of oxygen ions in the formation of a bifurcated current sheet in the magnetotail. *Journal of Geophysical Research: Space Physics*, *115*(A3), doi:10.1029/2009JA014710

Delamere, P.A., Otto, A., Ma, X., Bagenal, F. and Wilson, R.J., (2015). Magnetic flux circulation in the rotationally driven giant magnetospheres. *Journal of Geophysical Research: Space Physics*, *120*(6), pp.4229-4245. doi:10.1002/2015JA021036

Delcourt, D.C., Malova, H.V. and Zelenyi, L.M., (2006). Quasi adiabaticity in bifurcated current sheets. *Geophysical Research Letters*, *33*(6), doi:10.1029/2005GL025463

Dougherty, M.K., Kellock, S., Southwood, D.J., Balogh, A., Smith, E.J., Tsurutani, B.T., Gerlach, B., Glassmeier, K.H., Gleim, F., Russell, C.T. and Erdos, G., Neubauer F. M., Cowley S. W. H., (2004), The Cassini Magnetic Field Investigation, *Space Science Reviews*,*114*(1), 331–383, doi:10.1007/978-1-4020-2774-1

Dougherty, M.K., Cao, H., Khurana, K.K., Hunt, G.J., Provan, G., Kellock, S., Burton, M.E., Burk, T.A., Bunce, E.J., Cowley, S.W. and Kivelson, M.G., (2018). Saturn?s magnetic field revealed by the Cassini Grand Finale. *Science, 362*(6410). doi: 10.1126/science.aat5434

Felici, M., Arridge, C.S., Coates, A.J., Badman, S.V., Dougherty, M.K., Jackman, C.M., Kurth, W.S., Melin, H., Mitchell, D.G., Reisenfeld, D.B. and Sergis, N., (2016). Cassini observations of ionospheric plasma in Saturn's magnetotail lobes. *Journal of Geophysical Research: Space Physics*, *121*(1), 338-357, doi:10.1002/2015JA021648

Génot, V., Mottez, F., Fruit, G., Louarn, P., Sauvaud, J.A. and Balogh, A., (2005). Bifurcated current sheet: Model and Cluster observations. *Planetary and Space Science*, *53*(1-3), pp.229-235, doi:10.1016/j.pss.2004.09.048

Giampieri, G. and Dougherty, M.K., (2004). Modelling of the ring current in Saturn's magnetosphere. *Annales Geophysicæ 22* (2) 653-659, doi:10.5194/angeo-22-653-2004

Guo, R.L., Yao, Z.H., Wei, Y., Ray, L.C., Rae, I.J., Arridge, C.S., Coates, A.J., Delamere, P.A., Sergis, N., Kollmann, P. and Grodent, D., (2018). Rotationally driven magnetic reconnection in Saturn's dayside. *Nature Astronomy* 2, 640-645, doi:10.1038/s41550-018-0461-9

414 Harris, E. G., (1962). On a plasma sheath separating regions of oppositely directed magnetic
415 field, *Il Nuovo Cimento (1955-1965)*, *23*(1), 115–121, doi:10.1007/BF02733547
416 Hoshino, M., Nishida, A., Mukai, T., Saito, Y., Yamamoto, T. and Kokubun, S., 1996. Struc-
417 ture of plasma sheet in magnetotail: Double peaked electric current sheet. *Journal of Geo-*
418 *physical Research: Space Physics*, *101*(A11), pp.24775-24786, doi:10.1029/96JA02313
419 Israelevich, P.L. and Ershkovich, A.I., (2006). Bifurcation of Jovian magnetotail current
420 sheet. *Annales Geophysicae 24*6, 1479-1481, doi:10.5194/angeo-24-1479-2006
421 Israelevich, P.L., Ershkovich, A.I. and Oran, R., (2007). Bifurcation of the tail current
422 sheet in Jovian magnetosphere. Planetary and Space Science, 55(15), pp.2261-2266,
423 doi:10.1016/j.pss.2007.05.006
424 Israelevich, P.L. and Ershkovich, A.I., (2008). Bifurcation of the tail current sheet and ion
425 temperature anisotropy. *Annales geophysicae: atmospheres, hydrospheres and space sci-*
426 *ences* Vol. 26, No. 7, p. 1759, doi:10.5194/angeo-26-1759-2008
427 Jurac, S., McGrath, M.A., Johnson, R.E., Richardson, J.D., Vasyliunas, V.M. and Eviatar, A.,
428 2002. Saturn: Search for a missing water source. *Geophysical Research Letters*, *29*(24),
429 doi:10.1029/2002GL015855
430 Kellett, S., Bunce, E. J., Coates, A. J., Cowley, S. W. H., (2009). Thickness of Saturn's ring
431 current determined from north-south Cassini passes through the current layer, *Journal of*
432 *Geophysical Research*, *114*(A4), doi:10.1029/2008JA013942
433 Kellett, S., Arridge, C.S., Bunce, E.J., Coates, A.J., Cowley, S.W.H., Dougherty, M.K., Per-
434 soon, A.M., Sergis, N. and Wilson, R.J., (2011). Saturn's ring current: Local time de-
435 pendence and temporal variability. *Journal of Geophysical Research: Space Physics*,
436 *116*(A5),doi:10.1029/2010JA016216
437 Khurana, K.K., Kivelson, M.G.,(1989). On Jovian Plasma Sheet Structure, *Journal of Geo-*
438 *physical Research*, *94*(A9), 11,791–11,803, doi:10.1029/JA094iA09p11791
439 Khurana, K.K. (2001). Influence of solar wind on Jupiter's magnetosphere deduced from cur-
440 rents in the equatorial plane. *Journal of Geophysical Research: Space Physics*, *106*(A11),
441 25999-26016, doi:10.1029/2000JA000352
442 Kidder, A., Winglee, R.M. and Harnett, E.M., (2009). Regulation of the centrifugal inter-
443 change cycle in Saturn's inner magnetosphere. *Journal of Geophysical Research: Space*
444 *Physics*, *114*(A2), doi:10.1029/2008JA013100
445 Krupp, N., Dougherty, M. K., Woch, J., Seidel, R., Keppler, E., (1999). Energetic particles in
446 the duskside Jovian magnetosphere, *Geophysical Research Letters*, *34*(A11), 8779–8789,

447 doi:10.1029/1999JA900156

448 Martin, C. J. and Arridge, C. S., (2017). Cassini observations of aperiodic waves on Saturn's
449 equatorial current sheet. *Journal of Geophysical Research: Space Physics*, *122*(8) 8063-
450 8077,doi:10.1002/2017JA024293

451 Martin, C. J. and Arridge, C. S., (2018). Current Density in Saturn's equatorial current sheet:
452 Cassini magnetometer observations. *Journal of Geophysical Research: Space Physics 124*
453 279-292 doi:10.1029/2018JA025970

454 Matsui, T. and Daughton, W., 2008. Kinetic theory and simulation of collisionless tearing in
455 bifurcated current sheets. *Physics of Plasmas*, *15*(1), p.012901, doi:10.1063/1.2832679

456 Mok, C., Ryu, C.M., Yoon, P.H. and Lui, A.T., 2006. Global two fluid stability of bi-
457 furcated current sheets. *Journal of Geophysical Research: Space Physics*, *111*(A3),
458 doi:10.1029/2005JA011424

459 Nakamura, R., Baumjohann, W., Runov, A., Volwerk, M., Zhang, T.L., Klecker, B., Bog-
460 danova, Y., Roux, A., Balogh, A., Reme, H. and Sauvaud, J.A., (2002). Fast flow during
461 current sheet thinning. *Geophysical Research Letters*, *29*(23), doi:10.1029/2002GL016200

462 Paranicas, C.P., Mauk, B.H. and Krimigis, S.M., 1991. Pressure anisotropy and radial stress
463 balance in the Jovian neutral sheet. *Journal of Geophysical Research: Space Physics*,
464 *96*(A12), pp.21135-21140. doi:10.1029/91JA01647

465 Pontius, D. H., and T. W. Hill., (2006) Enceladus: A significant plasma source for Sat-
466 urn's magnetosphere. *Journal of Geophysical Research: Space Physics*, *111* (A9),
467 doi:10.1029/2006JA011674

468 Provan, G., Andrews, D. J., Arridge, C. S., Coates, A. J., Cowley, S. W. H., Cox, G.,
469 Dougherty, M. K., Jackman, C. M. (2012). Dual periodicities in planetary-period mag-
470 netic field oscillations in Saturn's tail. *Journal of Geophysical Research*, *117* A1,
471 doi:10.1029/2011JA017104

472 Ricci, P., Lapenta, G. and Brackbill, J.U., (2004). Structure of the magnetotail current: Ki-
473 netic simulation and comparison with satellite observations. *Geophysical Research Let-*
474 *ters*, *31*(6), doi:10.1029/2003GL019207

475 Runov, A., Nakamura, R., Baumjohann, W., Zhang, T.L., Volwerk, M., Eichelberger, H.U.
476 and Balogh, A., (2003). Cluster observation of a bifurcated current sheet. *Geophysical*
477 *Research Letters*, *30*(2), doi:10.1029/2002GL016136

478 Runov, A., Nakamura, R., Baumjohann, W., Treumann, R.A., Zhang, T.L., Volwerk, M.,
479 Vörös, Z., Balogh, A., Glaßmeier, K.H., Klecker, B. and Reme, H., 2003. Current sheet

structure near magnetic X-line observed by Cluster. *Geophysical Research Letters*, *30*(11), doi:10.1029/2002GL016730

Saito, M., 2015. THEMIS two point measurements of the cross tail current density: A thick bifurcated current sheet in the near Earth plasma sheet. *Journal of Geophysical Research: Space Physics*, *120*(8), pp.6258-6275, doi:10.1002/2015JA021142

Sergis, N., Jackman, C.M., Thomsen, M.F., Krimigis, S.M., Mitchell, D.G., Hamilton, D.C., Dougherty, M.K., Krupp, N., Wilson, RJ. (2017). Radial and local time structure of the Saturnian ring current, revealed by Cassini, *Journal of Geophysical Research: Space Physics*, *122*(2) 1803-1815, doi:10.1002/2016JA023742

Sitnov, M.I., Guzdar, P.N. and Swisdak, M., (2003). A model of the bifurcated current sheet. *Geophysical Research Letters*, *30*(13), doi:10.1029/2003GL017218

Sitnov, M.I., Swisdak, M., Drake, J.F., Guzdar, P.N. and Rogers, B.N., (2004). A model of the bifurcated current sheet: 2. Flapping motions. *Geophysical Research Letters*, *31*(9) doi:10.1029/2004GL019473

Sitnov, M.I. and Merkin, V.G., 2016. Generalized magnetotail equilibria: Effects of the dipole field, thin current sheets, and magnetic flux accumulation. *Journal of Geophysical Research: Space Physics*, *121*(8), 7664-7683, doi:10.1002/2016JA023001

Smith, E.J., Davis, L., Jones, D.E., Coleman, P.J., Colburn, D.S., Dyal, P. and Sonett, C.P., 1980. Saturn's magnetic field and magnetosphere. *Science*, *207*(4429), 407-410. doi:10.1126/science.207.4429.407

Sonnerup, B.Ö. and Cahill Jr, L.J., (1967). Magnetopause structure and attitude from Explorer 12 observations. *Journal of Geophysical Research*, *72*(1), 171-183, doi:10.1029/JZ072i001p00171

Southwood, D.J., Kivelson, M. G., (2001). A new perspective concerning the influence of the solar wind on the Jovian magnetosphere *Journal of Geophysical Research: Space Physics*, *106*(A4), doi:10.1029/2000JA000236

Thompson, S.M., Kivelson, M.G., El Alaoui, M., Balogh, A., Reme, H. and Kistler, L.M., (2006). Bifurcated current sheets: Statistics from Cluster magnetometer measurements. *Journal of Geophysical Research: Space Physics*, *111*(A3), doi:10.1029/2005JA011009

Thomsen, M. F., Jackman, C. M., Cowley, S. W. H., Jia, X., Kivelson, M. G. and Provan, G., (2016). Evidence for Periodic Variations in the Thickness of Saturn's Nightside Plasma Sheet, *Journal of Geophysical Research: Space Physics*, *122*(1), 280-292, doi:10.1002/2016JA023368

513 Tokar, R.L., Johnson, R.E., Thomsen, M.F., Delapp, D.M., Baragiola, R.A., Francis, M.F.,
514 Reisenfeld, D.B., Fish, B.A., Young, D.T., Crary, F.J. and Coates, A.J., 2005. Cassini ob-
515 servations of the thermal plasma in the vicinity of Saturn's main rings and the F and G
516 rings. *Geophysical Research Letters*, *32*(14), doi:10.1029/2005GL022690
517 Zelenyi, L.M., Delcourt, D.C., Malova, H.V. and Sharma, A.S., (2002). 'Aging'
518 of the magnetotail thin current sheets. *Geophysical Research Letters*, *29*(12),
519 doi:10.1029/2001GL013789
520 Zelenyi, L.M., Malova, H.V. and Popov, V.Y., (2003). Splitting of thin current sheets in the
521 Earth's magnetosphere. *Journal of Experimental and Theoretical Physics Letters*, *78*(5),
522 pp.296-299, doi:10.1134/1.1625728

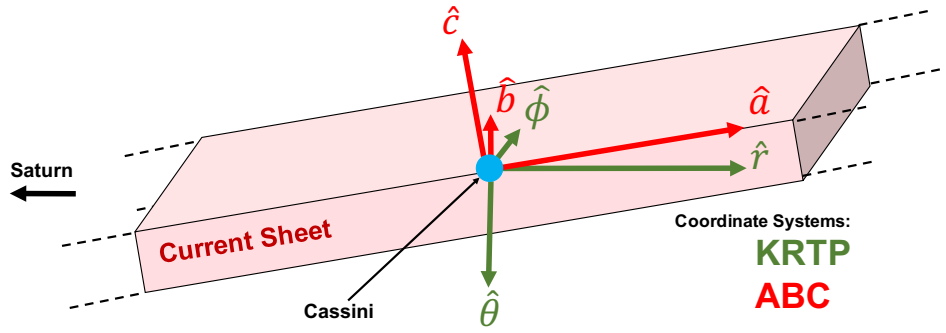

Figure 1. Cartoon of the relation between the current sheet coordinate system (ABC) and the KRTP (Kronian Radial, Theta, Phi) coordinates with respect to the current sheet and Saturn. KRTP is used here, however the method is independent of original co-ordinate system. KRTP is a spherical system with Saturn at the centre. The radial component is positive radially outwards from the planet, θ is positive southwards at the equator and ϕ is positive in the corotation direction.

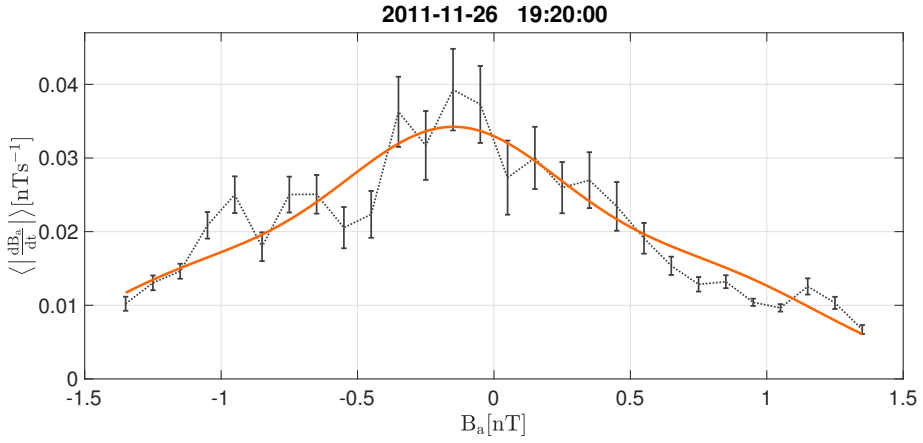

Figure 2. Proxies for the distance from the current sheet versus current sheet density for a Harris-like profile. The dotted line shows the mean of current density as a function of distance from the centre of the current sheet, with standard deviation shown by the error bars. The solid orange line is the fitted model of three Gaussians, where the central Gaussian is dominant and hence the example is a Harris-like current sheet. This example is found at 25.3 R_S and 13.5 SLT.

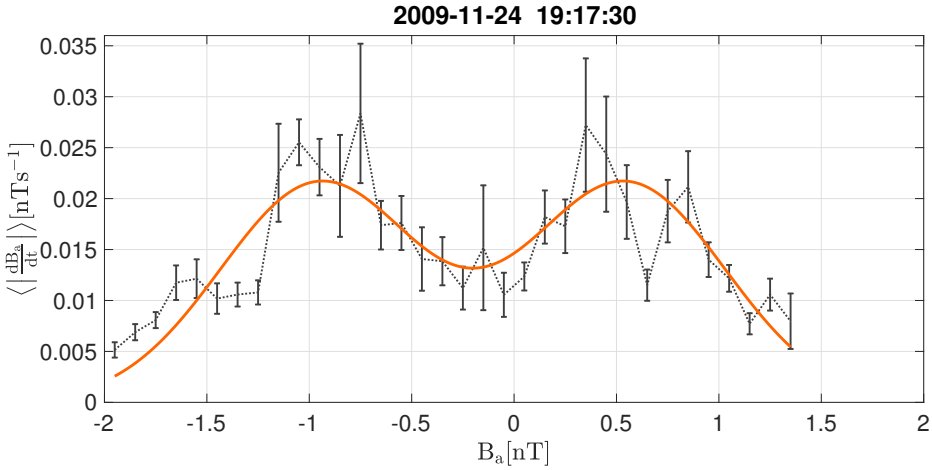

Figure 3. Proxies for the distance from the current sheet versus current sheet density for a bifurcated profile. The dotted line shows the mean of current density as a function of distance from the centre of the current sheet, with standard deviation shown by the error bars. The solid orange line is the fitted model of three Gaussians, where the peripheral Gaussians are dominant and hence the example is a bifurcated current sheet. This example is found at 30.5 R_S and 17.9 SLT.

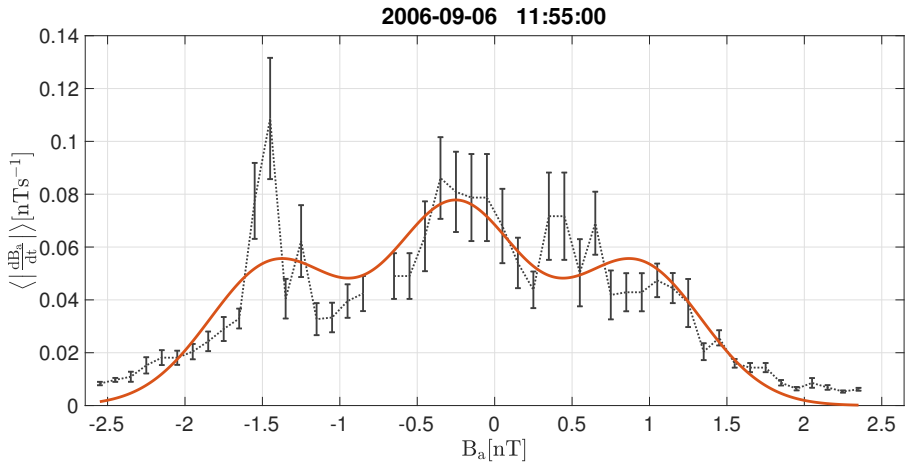

Figure 4. Proxies for the distance from the current sheet versus current sheet density for a unclassified/ambiguous profile. The dotted line shows the mean of current density as a function of distance from the centre of the current sheet, with standard deviation shown by the error bars. The solid orange line is the fitted model of three Gaussians, where the peripheral Gaussians are dominant and hence the example is a bifurcated current sheet. This example is found at 29.2 R_S and 1.6 SLT.

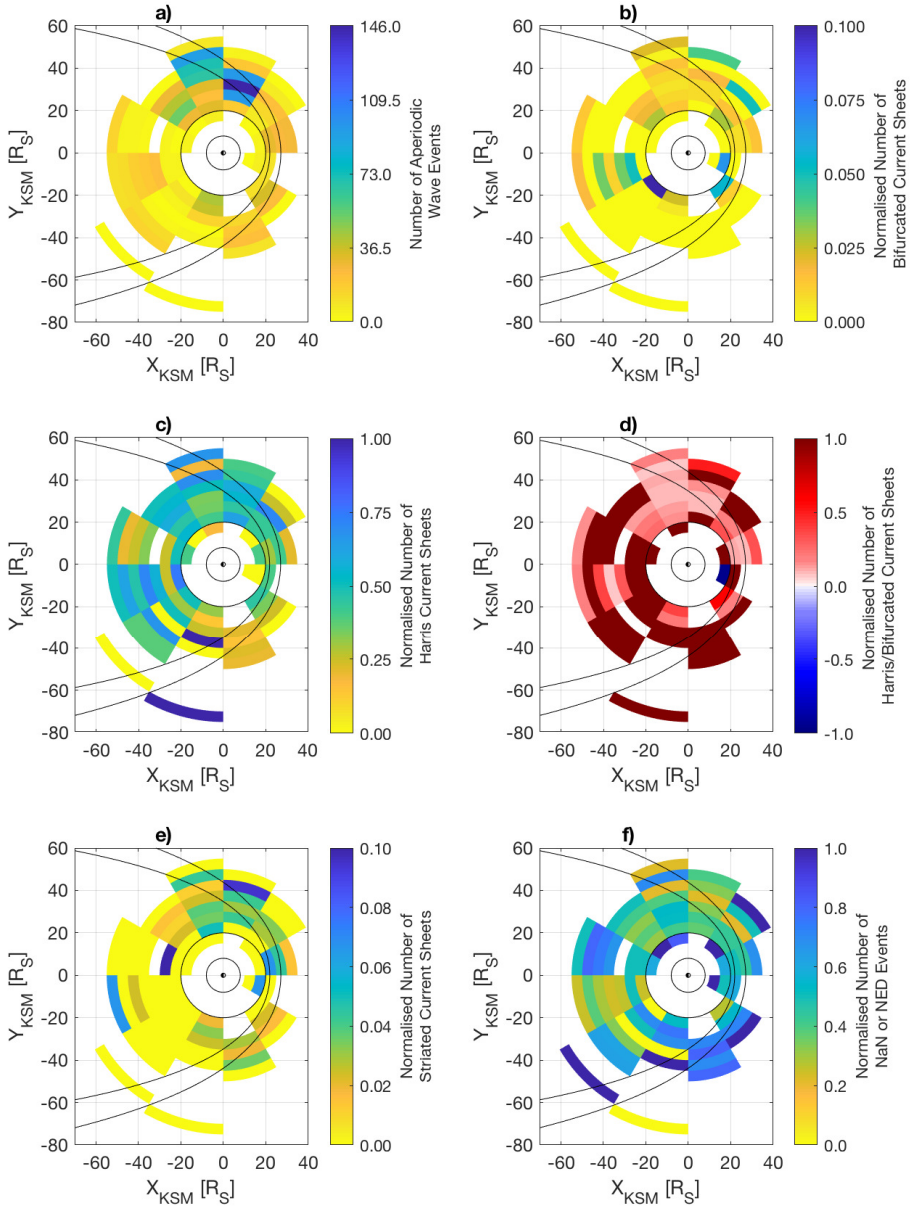

Figure 5. Distribution of total number of aperiodic wave events (a), number of bifurcated sheets normalised by total number of events (b) and number of Harris-like normalised by total number of events(c). d) shows the ratio of bifurcated to Harris-like current sheets. e) shows the number of unclassified or striated current sheets normalised by total number of events and the number of NaN and NED events normalised by total number of events is shown in f). Nominal magnetopause positions guide the eye in black, along with Titan's orbit at 20 R_S and Rhea's orbit at 9 R_S.